

Raman and TGA Study of Carbon Nanotubes Synthesized Over Mo/Fe Catalyst on Aluminium Oxide, Calcium Carbonate and Magnesium Oxide Support

EZEKIEL DIXON DIKIO*, NTAOTE DAVID SHOOTO,
FORCE TEFO THEMA and ABDULLAHI MOHAMED FARAH

Applied Chemistry and Nanoscience Laboratory, Department of Chemistry,
Faculty of Applied and Computer Science, Vaal University of Technology,
P.O Box X021, Vanderbijlpark, South Africa

ezeekield@vut.ac.za

Received 8 January 2013 / Accepted 14 February 2013

Abstract: Carbon nanomaterials were synthesized from Al_2O_3 , CaCO_3 and MgO used as support materials without a catalyst and over Mo/Fe catalyst on Al_2O_3 , CaCO_3 and MgO as support materials. The as-prepared nanomaterials were characterized by Raman spectroscopy, Thermogravimetric and Derivative thermogravimetric analysis (TGA & DTA). The intensity ratios (I_D/I_G), of the *D*- and *G*-bands were higher for Al_2O_3 , CaCO_3 and MgO as support materials and lower for Mo/Fe/ Al_2O_3 , Mo/Fe/ CaCO_3 and Mo/Fe/ MgO . The ratios of the sp^2/sp^3 bonded carbon were lower in the support than in the catalyst and support. TGA and DTA curves show MgO and Mo/Fe/ Al_2O_3 lost 37.39% and 11% mass respectively while Mo/Fe/ CaCO_3 and Mo/Fe/ MgO barely decomposed under high temperatures.

Keywords: Carbon nanotubes, Raman spectroscopy, Thermogravimetric analysis, Derivative thermogravimetric analysis, SEM, EDS, XRD

Introduction

There are widespread kinds of carbon nanostructures, but they all have a few elementary things in common. First, all of these nanostructures are primarily made up of the element carbon and all these artefacts are called carbon allotropes. The range of these materials starts with the well-known allotrope “graphite” and continues on to incorporate fullerenes, graphene and more complex structures such as carbon nanotubes¹.

Carbon nanomaterials have given the material sciences and the chemistry of carbon a new direction in recent years. Different carbon nanomaterials offer an extensive range of beneficial properties relating to electrical conductivity, thermal resistance, and exceptional strength, making them attention-grabbing materials to a broad range of industries².

Carbon nanotubes were found³ by scientific observation in 1991. Carbon nanotubes are molecular scale tubes of graphitic carbon with outstanding properties. They are among the

stiffest and strongest fibres known and have remarkable optical, electronic and mechanical properties and many other unique characteristics⁴. For these reasons they have attracted considerable academic and industrial interest and worldwide attention in both fundamental and technological perspectives owing to their broader-scope of interested properties⁵.

Many different methods have been employed for the synthesis of (CNTs), methods such as chemical vapor deposition (CVD)^{6,7}, laser ablation^{8,9} and arch discharge^{10,11}. Since catalytic chemical vapor deposition (CVD) is a simple and relatively cheap technique, it might be the most promising method for large-scale production of carbon nanotubes under reasonably mild conditions. Additionally, with the CVD method, the growth of carbon nanotubes like selectivity of other catalytic reaction can be successfully controlled by adjusting the reaction conditions and preparing proper catalyst¹².

Raman spectroscopy is a simple and powerful technique to identify and study different types of carbon nanotubes it generates data pertaining to the purity, defects, tube alignment and assist in distinguishing between the presence of carbon nanotubes and relative carbon allotropes. Thermogravimetric analysis, (TGA) determines the mass change of a substance measured as function of temperature whilst the substance is subjected to a controlled temperature programme. It has been found a single metal and mixture of metals supported on oxides, clays or zeolites have great contribution in terms of catalytic activity to nanotubes synthesis¹³⁻¹⁵. Dispersion and stabilization of the metallic catalyst materials can also be performed by using a number of oxides and mixed oxides. It is well known that the catalytic properties of the catalyst-support material combine strongly depending on the interaction between catalyst and the support material.

In this paper we present Raman and thermogravimetric analysis of carbon nanotubes synthesized in a CCVD reactor over molybdenum and iron catalyst supported on aluminium oxide (Al_2O_3), calcium carbonate (CaCO_3) and magnesium oxide (MgO). Nanomaterial obtained from the support materials only, aluminium oxide, calcium carbonate and magnesium oxide, without a catalyst, were also studied to identity the effect of the support on the as-prepared carbon nanotube. The as-prepared nanomaterial were characterized by SEM, EDS, TEM and XRD.

Experimental

All chemicals used in this research were of analytical grade. All solutions were prepared with deionized water. All chemicals were purchased from sigma-Aldrich and no further purification were performed on the chemicals, they were all used as they were from the manufacturer.

Preparation of catalyst

A mixture of ammonium molybdate ($(\text{NH}_4)_5\text{Mo}_7\cdot 4\text{H}_2\text{O}$), citric acid ($\text{C}_6\text{H}_8\text{O}_7\cdot \text{H}_2\text{O}$) and iron(III) nitrate ($\text{Fe}(\text{NO}_3)_3$) respective masses 0.074 g, 4.266 g and 1.647 g were dissolved in 50 mL de-ionized water in a beaker¹⁶⁻¹⁹. A mixture was gently heated at 50 °C to avoid splatter; solution was heated up to a time that it crystalized. The formed crystals were placed in an oven and baked at 150 °C over-night (12 h). Hard solid crystals were crashed into power.

Synthesis of carbon nanotubes

Catalytic chemical vapour deposition method was used the synthesis of carbon nanotubes. The reactor consists of a tube furnace with a quartz tube 70 cm long and 40 mm diameter, and temperature controller. The catalyst was placed on a quartz boat and placed in the middle

of the quartz tube then inserted in the furnace. The furnace was heated for 85 min. at a rate 10 °C/min. in an inert atmosphere of nitrogen gas, to reach the desired temperature (85 °C) once reached the target temperature was kept constant at 850 °C. Then a mixture of acetylene (C₂H₂), at a flow rate of 45 mL/min and nitrogen at 150 mL/min was introduced into the quartz tube for 80 min for the fabrication of carbon nanotubes. After the reaction had ceased the quartz tube was cooled to room temperature in a nitrogen atmosphere, and graphitic crystalline carbon was collected for characterization.

Characterization

The morphological features of the as-prepared carbon nanotubes were analyzed by Raman spectroscopy and Thermogravimetric analyser. The Raman spectra were obtained by a Raman spectroscopy, Jobin-Yvon HR800 UV-Vis-NIR Raman spectrometer equipped with an Olympus BX 40 attachment. The excitation wavelength was 514.5 nm with an energy setting of 1.2 mV from a coherent Innova model 308 argon-ion laser. The Raman spectra were collected by means of back scattering geometry with an acquisition time of 50 seconds. The surface morphology, SEM and EDS measurements were recorded with a JEOL 7500F Field Emission scanning electron microscope. The HR-TEM images of the sample were obtained by a CM 200 electron microscope operated at 100 kV. The thermal behaviour of the carbon nanotube and the catalyst were investigated by TGA using a Perkin Elmer Simultaneous Thermal Analyzer (STA 6000) under a nitrogen environment. The as-prepared carbon nanotube sample was heated in platinum crucibles with nitrogen gas flow rate of 19.7 mL/min and a gas pressure of 4.0 bars. The dynamic measurement was made from 30 °C and 950 °C with a ramp rate of 30 °C/min to 900 °C. Powder X-ray diffraction (PXRD) patterns were collected with a Bruker AXS D8 Advanced diffractometer operated at 45 kV and 40 mA with monochromated copper K α 1 radiation of wavelength ($\lambda = 1.540598$) and K α 2 radiation of wavelength ($\lambda = 1.544426$). Scan speed of 1 s/step and a step size of 0.03°.

Results and Discussion

Raman spectroscopy is an elementary technique used to identify and study different kinds of carbon nanotubes, it yields information about the purity, defects and contributes in the distinction of carbon nanotubes and other carbonaceous materials. The support materials, aluminium oxide, calcium carbonate and magnesium oxide without catalyst were placed in the CCVD reactor separately with acetylene and nitrogen gas passed over the support as it is heated. After the samples were cooled, the as-prepared material were analysed by Raman spectroscopy. The Raman spectra for the as-prepared carbon nanomaterial obtained with the support material in the absence of a catalyst is presented in Figure 1(a-c). Table 1 show the peak height and intensity of the *T*-, *D*- and *G*-bands and their I_D/I_G ratios. The Raman spectra of the support material only show characteristic bands of multiwall carbon nanotubes. Three bands are observed at 1121, 1339 and 1588 cm⁻¹ for aluminium oxide, Figure 1(a), at 1122, 1301 and 1562 cm⁻¹ for calcium carbonate, Figure 1(b) and at 1122, 1318 and 1566 cm⁻¹ for magnesium oxide, Figure 1(c). The peak observed at 1121, 1122 and 1122 cm⁻¹ in the spectra for aluminium oxide, calcium carbonate and magnesium oxide respectively is assigned as T-band originating from *sp*³ bonded carbon and it is sensitive to small changes in *sp*³ content²⁰. The peak at 1339, 1301 and 1318 cm⁻¹ in the spectra for aluminium oxide, calcium carbonate and magnesium oxide respectively correspond to the *D*-band of disordered graphitic carbon in carbon nanotubes. The peak at 1588, 1562 and 1566 cm⁻¹ in the spectra for aluminium oxide, calcium carbonate and magnesium oxide respectively corresponds to the *G*-band of graphitic carbon in carbon nanotubes. The *D*- and *G*-bands

indicate the presence of crystalline graphitic carbon in carbon nanotubes. The presence of these two peaks is evidence that the support material could be used as a catalyst in itself in the synthesis of carbon nanotubes. The *D*-bands have been attributed to the presence of amorphous carbon due to surface defects of carbon nanotubes while the *G*-bands are due to the presence of ordered graphitic carbon nanotubes in the prepared samples. The *D*- and *G*-bands in the Raman spectra produce an overtone which resonates at about 2600 cm^{-1} . No overtone is observed in the Raman spectra of the support materials, indicating the low quality of carbon nanotubes synthesized. The intensity ratio of the two peaks, (I_D/I_G), considered a parameter in characterizing the quality of carbon nanotubes synthesized, a higher intensity ratio indicate a higher degree of disorder in the carbon nanotube. The intensity ratio for the two peaks in aluminium oxide and magnesium oxide, Figure 1(a) and (c) are 1.142 and 1.014 respectively, indicating the presence of low quality carbon nanotubes. The (I_D/I_G) for calcium carbonate, Figure 1(b), of 0.056 show the presence of high quality carbon nanotube. The low height of the peak show very low quantity of carbon nanotubes was formed.

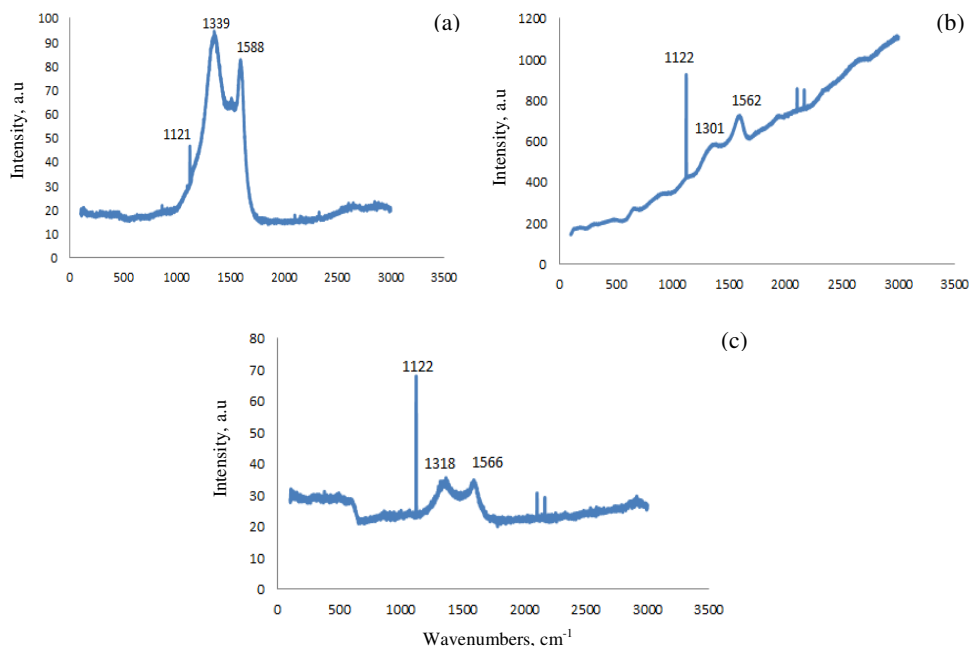


Figure 1. Raman spectra of support material only used in the synthesis of carbon nanotubes without a catalyst, (a) aluminium oxide, (b) calcium carbonate and (c) magnesium oxide

Table 1. Table of *T*-band peak height and intensity, *D*- and *G*-band peak height and intensity and ratio of *D*- and *G*-bands obtained from Raman spectra of carbon nanotube synthesized with catalyst support only

Support material	<i>T</i> -Band		<i>D</i> -Band		<i>G</i> -Band		I_D/I_G
	Peak, cm^{-1}	Intensity, au	Peak, cm^{-1}	Intensity, au	Peak, cm^{-1}	Intensity, au	
Al_2O_3	1121	44.45	1339	92.15	1588	80.66	1.142
CaCO_3	1122	542.5	1301	8.6	1562	153.0	0.056
MgO	1122	67.94	1318	33.49	1566	33.04	1.014

The Raman spectra of the as-prepared carbon nanomaterial with Mo/Fe catalyst on aluminium oxide, calcium carbonate and magnesium oxide support respectively are presented in Figure 2 (a-c). Table 2 show peak heights and intensity of the *D*- and *G*-bands, the peak height and intensity of the overtone band and the intensity ratio of the *D*- and *G*-bands. The Raman spectra for the supported catalyst, show peaks at 1332, 1343 and 1581 cm^{-1} respectively, that corresponds to the *D*-band of graphitic carbon. The *G*-band that indicates the presence of ordered graphitic carbon nanotubes are observed at 1581, 1576 and 1585 cm^{-1} respectively²¹. The presence of the *D*- and *G*-bands in the as-prepared sample strongly suggests the presence amorphous and ordered graphitic carbon in the sample. An overtone peak is observed in the spectra for Mo/Fe/CaCO₃, figure 2(b) at 2670 cm^{-1} . The presence of this resonance peak in the synthesis could be related to the amount of carbon nanotubes produced as well as their purity. The absence of this resonance peak in the as-prepared carbon nanomaterial obtained from Mo/Fe/Al₂O₃ and Mo/Fe/MgO, Figure 2(a & c) and its presence in the as-prepared carbon nanomaterial synthesized from the catalyst system Mo/Fe/CaCO₃, Figure 2(b), is an indication that the catalyst system Mo/Fe/CaCO₃, produced a better and purer yield of carbon nanotubes compared to the others. The intensity ratio of the two peaks, (I_D/I_G), which provide insight regarding the quality of carbon nanotube synthesized are found to be 1.0533 for Mo/Fe/Al₂O₃, 0.9953 for Mo/Fe/CaCO₃ and 0.9748 for Mo/Fe/MgO. A high intensity ratio indicates a high degree of disorder in the carbon nanotube synthesized. This data again confirms the quality of the nanomaterial produced from the catalyst system Mo/Fe/CaCO₃. The spectra of the as-prepared sample obtained with the catalyst over calcium carbonate support, Figure 2(b), in addition to the *D*- and *G*-bands and the overtone peak, show additional peaks at 213, 276 and 377 cm^{-1} .

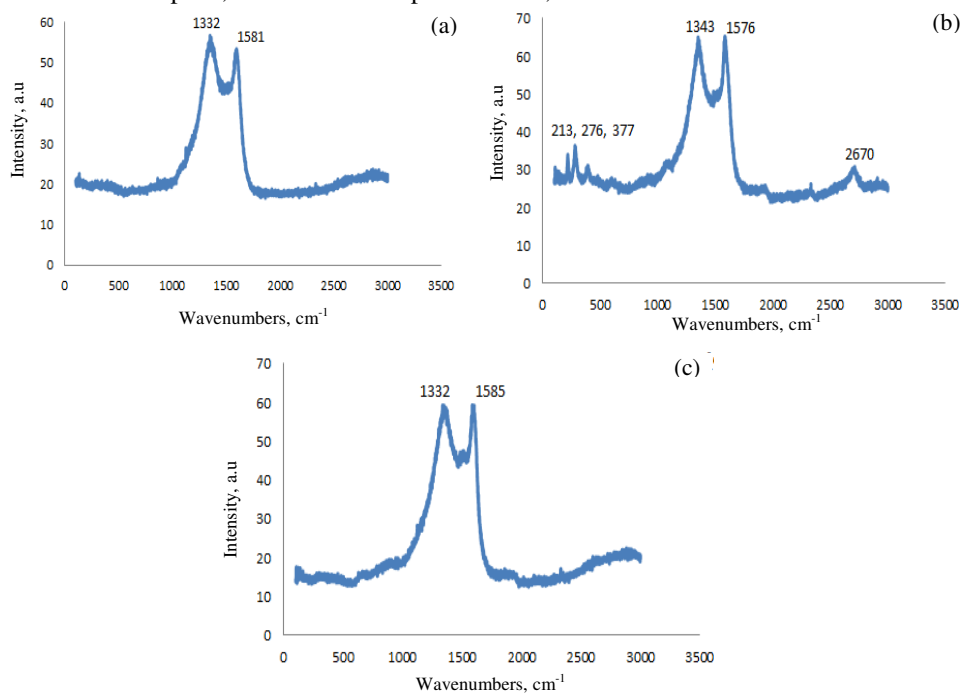


Figure 2. Raman spectra of carbon nanomaterial synthesized with Mo/Fe catalyst on (a) aluminium oxide, (b) calcium carbonate and (c) magnesium oxide support

Table 2. Table of *D*- and *G*-band peak height and intensity, overtone band peak height and intensity and ratio of *D*- and *G*-bands obtained from Raman spectra of carbon nanotube synthesized with Mo/Fe catalyst on different support

Catalyst and support	<i>D</i> -Band		<i>G</i> -Band		Overtone-band		I_D/I_G
	Peak cm^{-1}	Intensity, au	Peak, cm^{-1}	Intensity, au	Peak, cm^{-1}	Intensity, au	
Mo/Fe/ Al_2O_3	1332	55.17	1581	52.38	-	-	1.0533
Mo/Fe/ CaCO_3	1343	63.34	1576	63.64	2670	28.95	0.9953
Mo/Fe/MgO	1332	57.75	1585	59.24	-	-	0.9748

A comparison of the Raman spectra of the support material with the catalyst and support show the scope of interaction between the support and the catalyst. We observe that in the absence of the catalyst, aluminium oxide, calcium carbonate and magnesium oxide supports, Figure 1(a-c), produce a significant peak at 1121 and 1122 cm^{-1} , which is absent in the spectra of the catalyst and support, Figure 2(a-c). The presence of the catalyst in the synthesis provides an interaction that eliminates this peak. This peak at 1121 and 1122 cm^{-1} is most prominent in the spectra for calcium carbonate and magnesium oxide supports. The Raman spectra of the support material with the catalyst and support show shifts in the *D*- and *G*-bands. In the support materials, the *D*- and *G*-bands are observed at low wavenumbers while in the spectra of the catalyst and support, the *D*- and *G*-bands are observed at higher wavenumbers. The change in the resonance wavenumbers show the presence of sp^2 bonded carbon atoms in the as-prepared sample. Using the 514.5 nm laser excitation, and the McNamara *et al* formula:²²

$$f = \frac{100 \times I_G}{75 \times I_D + I_G}$$

Where I_D is the intensity of the *D*-band at about 1332 cm^{-1} and I_G is the intensity of the *G*-band at about 1550 cm^{-1} attributed to C=C sp^2 bond stretching mode and f is the sp^2/sp^3 bond ratio. The sp^2/sp^3 ratio bond for the as-prepared nanomaterial on a support without a catalyst and that of catalyst with support is presented in Figure 3. The figure show the ratio of sp^2/sp^3 bonded carbon to be highest in calcium carbonate and lowest in aluminium in the as-prepared nanomaterial without a catalyst. With the as-prepared nanomaterial on a catalyst and support, the ratio is highest in Mo/Fe/MgO and lowest in Mo/Fe/ Al_2O_3 .

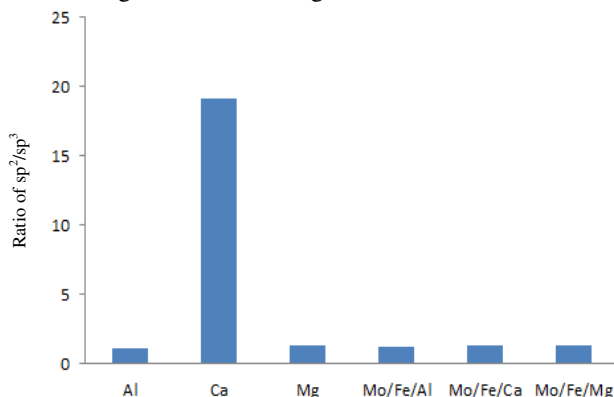


Figure 3. Ratio of sp^2/sp^3 bonded carbon present in the as-prepared carbon nanomaterial.

TGA analysis was employed to examine the thermal stability of the as-prepared carbon nanomaterial obtained from Mo/Fe catalyst on aluminium oxide, calcium carbonate and magnesium oxide support and the as-prepared carbon nanomaterial without catalyst. Thermogravimetric (TGA) and the derivative thermogravimetric (DTG) curve of the weight loss are in most instances used to investigate the presence of carbon nanotubes. The interpretations of these curves are not straight forward due to the presence of catalyst particles during weight loss analysis. The temperature at which carbon nanomaterials are oxidized is an index of their stability. Thermogravimetric and derivative thermogravimetric analysis of support materials, aluminium oxide, calcium carbonate and magnesium oxide are presented in Figure 4(a-c). The thermogravimetric analysis of aluminium oxide and calcium carbonate, Figure 4(a & b), show weight loss of about 7%. The TGA curve decreases steadily from the start without any exothermic or endothermic reaction. The derivative thermogravimetric analysis (DTA), curve show no thermal event taking place in the analysis showing a straight line curve. The thermogravimetric and derivative thermogravimetric analysis for magnesium oxide, Figure 4(c), on the other hand show a weight loss of 37.39%. The weight loss started from 601.35-831.83 °C indicating decomposition of formed carbonaceous material. The DTA show an endothermic peak at 692.89 °C corresponding to a single decomposition reaction.

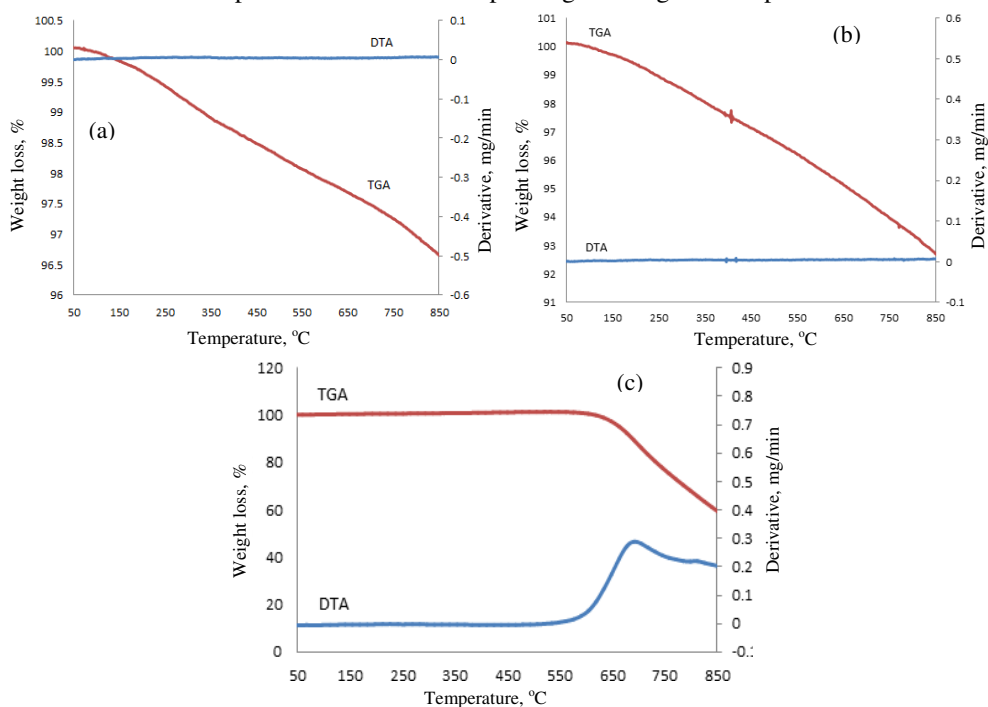


Figure 4. Thermogravimetric and derivative thermogravimetric analysis of as-prepared carbon nanomaterial obtained from support material from 50-850 °C. (a) Aluminium oxide, (b) calcium carbonate and (c) magnesium oxide

Thermogravimetric and derivative thermogravimetric analysis of carbon nanomaterial obtained with the catalyst Mo/Fe supported on aluminium oxide, calcium carbonate and magnesium oxide are presented in Figure 5(a-c). The TGA curve for Mo/Fe/Al₂O₃, Figure 5(a), shows a one-step decomposition reaction. Weight loss started at 521.6 °C and ended at 687.7 °C

giving rise to 11% weight loss. The derivative thermogravimetric analysis (DTA) show a single endothermic peak at 608 °C. The product show high stability and the low weight loss indicate the presence of low amorphous soot in the product. The TGA curve for Mo/Fe/CaCO₃, Figure 5(b), shows a gradual decrease in temperature from the start to 700 °C. A small decomposition reaction from 353.21-392.02 °C, which did not produce either an endothermic or exothermic change in the DTA curve, is observed. The TGA curve for Mo/Fe/MgO, Figure 5(c), shows a gradual decrease in temperature from the start to 800 °C. Neither decomposition reaction nor an endothermic or exothermic change in the DTA curve, is observed.

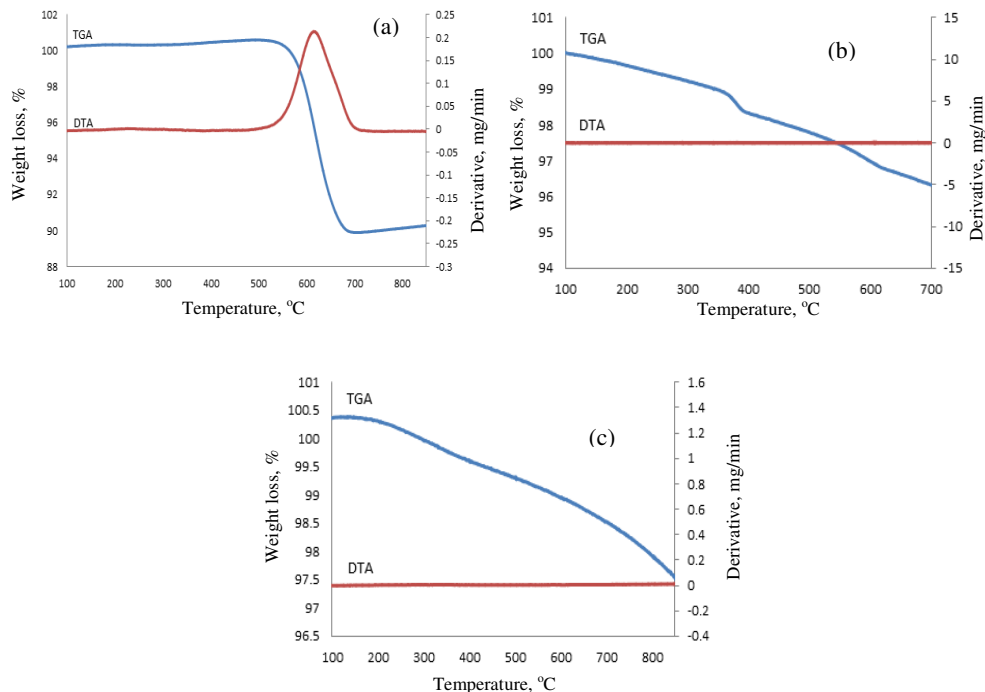


Figure 5. Thermogravimetric and derivative thermogravimetric analysis of as-prepared carbon nanomaterial obtained from the catalyst Mo/Fe supported on (a) aluminium oxide, (b) calcium carbonate and (c) magnesium oxide

Scanning electron microscope of as prepared carbon nanomaterial obtained with support materials only and catalysts on support material are presented in Figure 6 and 7. The images show a few strands of nanomaterial obtained from the synthesis procedure. These strands of nanomaterial support the Raman spectra result that indicated the presence of D- and G- bands in the as-prepared samples that suggests the presence amorphous and ordered graphitic carbon. Nanospheres and nanotubes are observed in Figure 7(c) when Mo/Fe supported on magnesium oxide is used in the synthesis.

Energy dispersive spectroscopy (EDS) of the Mo/Fe catalyst supported on aluminium oxide, calcium carbonate and magnesium oxide are presented in Figure 8. All spectra show the presence of the elements carbon, oxygen and the elements aluminium, Figure 8(a), calcium, Figure 8(b) and magnesium, Figure 8(c). These spectra give credence to the presence of carbon nanomaterial formed in the synthesis. The intensity of the carbon peak in Figure 8(a-c) is in agreement with the scanning electron micrograph result, Figure 7(a-c), that show the amount of carbon nanomaterial formed.

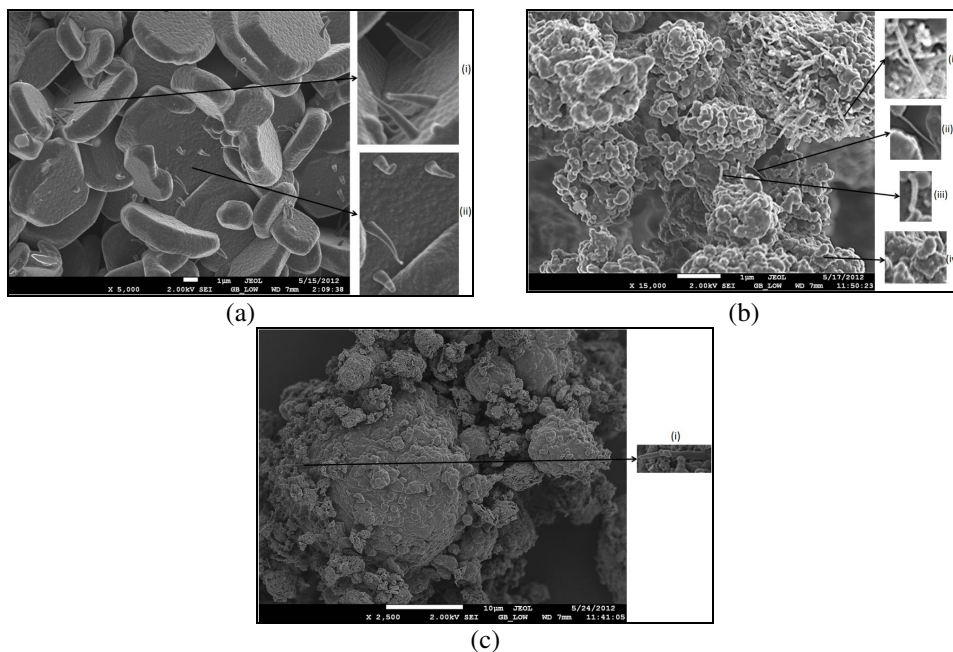


Figure 6. Scanning Electron Microscope (SEM) of as-prepared carbon nanomaterial obtained from support material from 50-850 °C. (a) Aluminium oxide, (b) calcium carbonate and (c) magnesium oxide

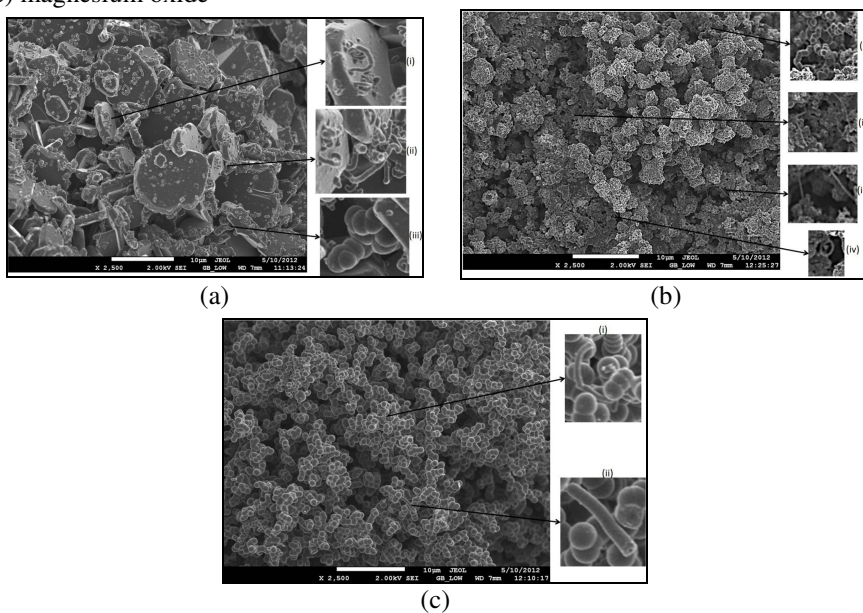


Figure 7. Scanning Electron Microscope (SEM) analysis of as-prepared carbon nanomaterial obtained from the catalyst Mo/Fe supported on (a) aluminium oxide, (b) calcium carbonate and (c) magnesium oxide

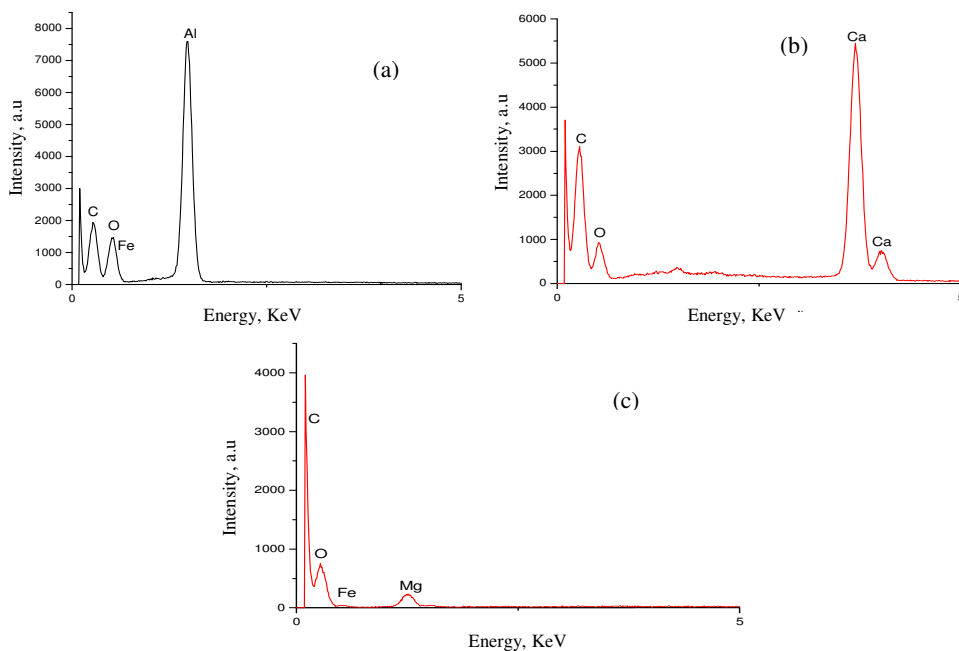


Figure 8. Energy Dispersive Spectroscopic (EDS) analysis of as-prepared carbon nanomaterial obtained from the catalyst Mo/Fe supported on (a) aluminimum oxide, (b) calcium carbonate and (c) magnesium oxide.

Figure 9 show the transmission electron micrograph (TEM) of nanomaterial obtained from the catalyst Mo/Fe supported on aluminimum oxide, calcium carbonate and magnesium oxide. Figure 9 (b and c) show cylindrical nanotubes with inset that indicate the lattice structure of the nanotubes formed in the synthesis.

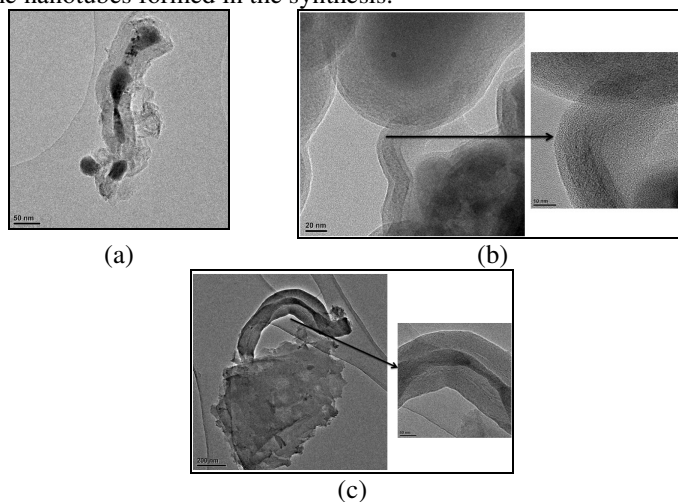


Figure 9. Transmission Electron Microscope (TEM) analysis of as-prepared carbon nanomaterial obtained from the catalyst Mo/Fe supported on (a) aluminimum oxide, (b) calcium carbonate and (c) magnesium oxide

X ray diffraction (XRD) of as prepared carbon nanomaterials obtained with support materials only and catalysts on aluminium oxide, calcium carbonate and magnesium oxide as support material are presented in Figure 10 and 11. The diffractogram presented in Figure 10(a-c) show several Bragg diffraction peaks with the most notable at $2\theta = 22.79^\circ$, 24.18° and 42.83° . The peaks at $2\theta = 22.79^\circ$, 24.18° and 42.83° correspond to hexagonal graphite lattice of multi-walled carbon nanotubes. The peaks at $2\theta = 22.79^\circ$ and 24.18° , Figure 10(b and c) are low intensity peaks which indicate the presence of small amounts of amorphous material in association with nanotubes. The high intensity of the peak at $2\theta = 42.83^\circ$, Figure 10(c), is an indication of the high quality of carbon nanomaterial present in the as-prepared carbon nanomaterial. The diffraction presented in Figure 11(a-c) also show several Bragg diffraction peaks with the most notable at $2\theta = 23.50^\circ$, 23.71° and 42.80° . The peaks at $2\theta = 23.50^\circ$ and 23.71° , Figure 11(b and c) are low intensity peaks which indicate the presence of small amounts of amorphous material in association with nanotubes. The high intensity of the peak at $2\theta = 42.80^\circ$, Figure 11(c), is an indication of the high quality of carbon nanomaterial present in the as-prepared carbon nanomaterial.

A comparison of the XRD peaks obtained from the as prepared carbon nanomaterials obtained with support materials only and catalysts on aluminium oxide, calcium carbonate and magnesium oxide as support material are presented in Table 3 and 4. The tables show the shifts in the Bragg diffraction peaks and intensity for the carbon nanomaterial obtained in the synthesis.

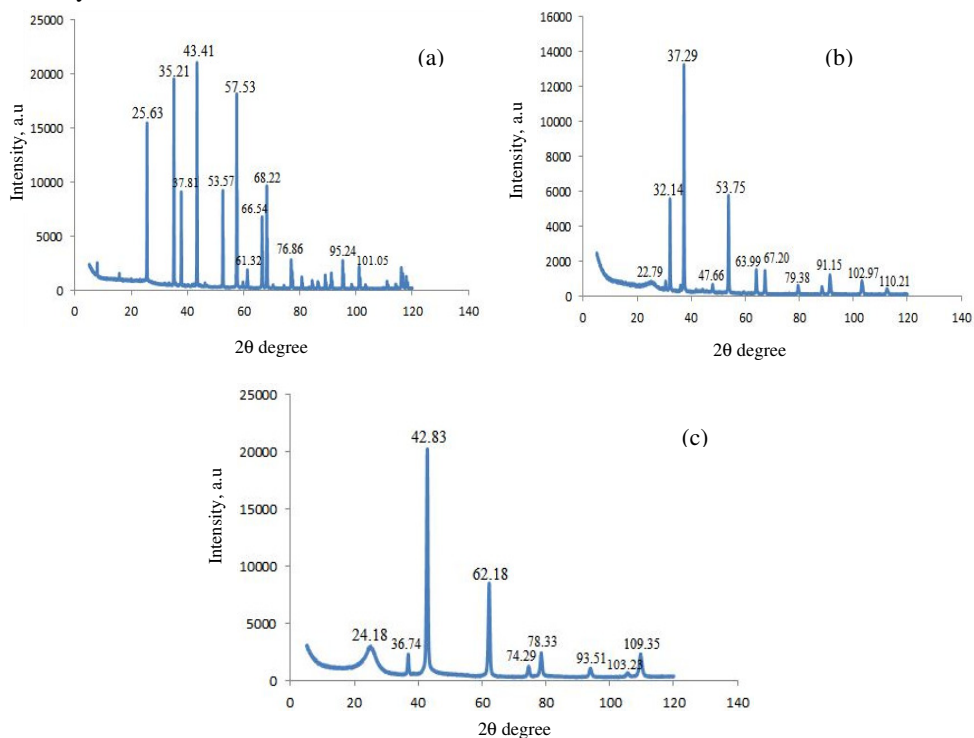


Figure 10. X-Ray Diffraction (XRD) analysis of as-prepared carbon nanomaterial obtained from support material from 50-850 °C. (a) Aluminium oxide, (b) calcium carbonate and (c) magnesium oxide

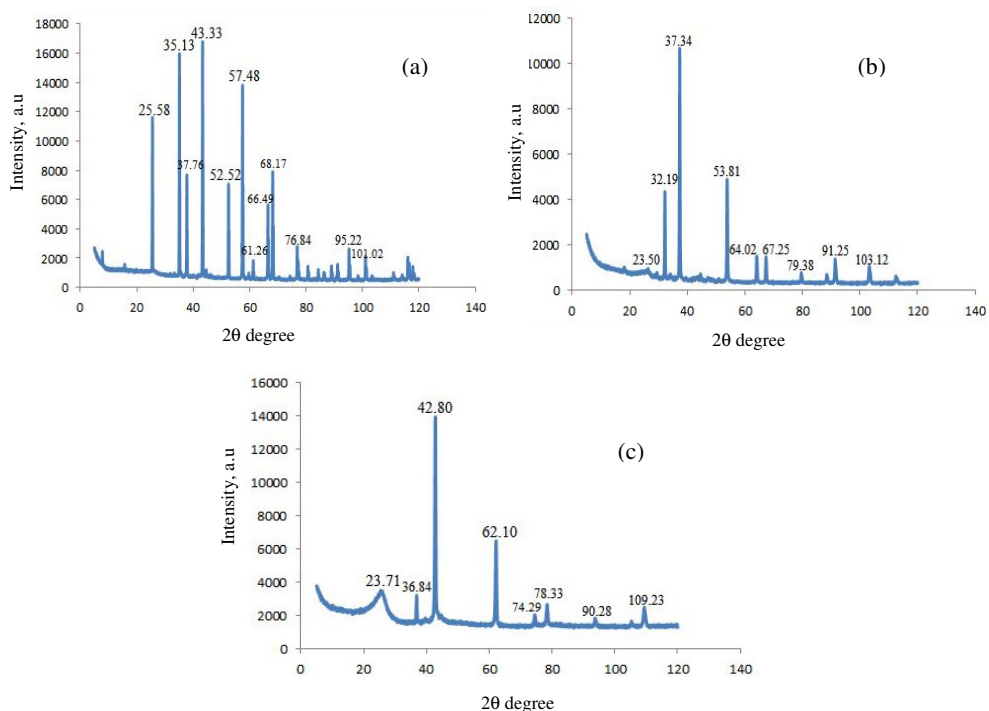


Figure 11. X-ray Diffraction (XRD) analysis of as-prepared carbon nanomaterial obtained from the catalyst Mo/Fe supported on (a) aluminium oxide, (b) calcium carbonate and (c) magnesium oxide

Table 3. Comparison XRD peaks obtained from as-prepared carbon nanotubes from Al_2O_3 , CaCO_3 and MgO

Sample name	Amorphous carbon		Nanomaterial	
	2 Theta, degree	Intensity, a.u	2 Theta, degrees	Intensity, a.u
Al_2O_3	25.63	15492	43.41	20703
CaCO_3	22.79	646	37.29	13227
MgO	24.18	2351	42.83	19937

Table 4. Comparison XRD peaks obtained from as-prepared carbon nanotubes from Mo/Fe/ Al_2O_3 , Mo/Fe/ CaCO_3 and Mo/Fe/ MgO

Sample name	Amorphous Carbon		Nanomaterial	
	2theta, degree	Intensity, a.u	2 Theta, degrees	Intensity, a.u
Mo/Fe/ Al_2O_3	25.58°	11553	43.33°	16756
Mo/Fe/ CaCO_3	23.50°	817	37.34°	10664
Mo/Fe/ MgO	23.71°	3096	42.80°	13710

Conclusion

In summary, carbon nanomaterials were synthesized with catalyst on support material and with support and no catalyst. The support material without catalyst produced nanomaterial with sp^2/sp^3 bonded carbon and carbonaceous material as observed in the *D*- and *G*-bands. Raman spectra of carbon nanomaterial obtained from Al_2O_3 , CaCO_3 and MgO without catalyst

showed significantly the presence of poor quality carbon nanotubes with high defects levels hence the intensity ratio, (I_D/I_G), for Al_2O_3 and MgO was found to be 1.142 and 1.014 respectively, on the other hand, Raman spectra carbon nanomaterial obtained from $CaCO_3$ gave evidence for the presence of high quality carbon nanomaterial with less defects with intensity ratio 0.056. Raman spectra for nanomaterial synthesized with catalyst and support, Mo/Fe/ Al_2O_3 , Mo/Fe/ $CaCO_3$ and Mo/Fe/MgO show the influence of the catalyst in the synthesis. The peaks for the D- and G-bands were shifted to higher wavenumbers. The intensity ratios, (I_D/I_G), were lower than that obtained from the support only. The sp^2/sp^3 bonded carbon ratios were significantly low. TGA and DTA curves of the carbon nanomaterial from Al_2O_3 and $CaCO_3$ show partial decomposition when subjected to high temperatures, while MgO lost about 37,39% of its mass indicating decomposition of synthesized carbonaceous materials. Mo/Fe/ $CaCO_3$ and Mo/Fe/MgO barely decomposed under high temperatures while Mo/Fe/ Al_2O_3 lost 11% of its mass. The presence of catalyst stabilised and assisted in the synthesis of carbon nanomaterial. Scanning electron microscope and X-ray diffraction confirm the presence of carbon nanomaterial and an indication of the amount produced.

Acknowledgment

This work was supported by a research grant from the Faculty of Applied and Computer Science Research and Publications Committee of Vaal University of Technology, Vanderbijlpark.

References

1. Mehn D, Fonseca A, Bister G and Nagy J B, *Chem Phys Lett.*, 2004, **393**(4-6), 378-384.
2. Bouanis F B, Baraton L, Huc V, Pribat D and Cojocar C S, *Thin Solid Films.*, 2011, **519**(14), 4594-4597.
3. Iijima S, *Nature*, 1999, **56**, 354-356.
4. Chaisitsak S, Yamada A and Konagai M, *Diamond Relat Mater.*, 2004, **13**(3), 438-444.
5. Jayatissa A H and Guo K. *Vacuum*, 2009, **83**(5), 853-856.
6. Chadderton L T and Ying Chen, *Phys Lett A*, 1991, **263**(4-6), 401-405.
7. Kong J, Cassell A M and Dai H, *Chem Phys Lett.*, 1998, **292**(6), 567-574.
8. Yang H, Mercier P, Wang S C and Akins D L, *Chem Phys Lett.*, 2005, **416**, 18-21.
9. Dai H, *Surf Sci.*, 2002, **500**(1-3), 218-241.
10. Dresselhaus M S, Dresselhaus G and Saito R, *Carbon*, 1995, **33**(7), 883-891.
11. He R R, Jin H Z, Zhu J, Yan Y J and Chen X H, *Chem Phys Lett.*, 1998, **298**(1-3), 170-176.
12. Dikio E D, *J Chem.*, 2011, **8**(3), 1014-1021.
13. Thaib A, Martin G A, Pinheiro P, Schouler M C and Gadelle P, *Catal Lett.*, 1999, **63**(3-4), 135-141.
14. Konya Z, Nagaraju N, Tamasi A, Mukhopadhyay K M, Fonseca A and Nagy J B, Electrical properties of Nanomaterials-Science and Technology of Molecular Structures: Kuzmany H, Fink J, Mehring M and Roth S, Eds., American Institute of Physics, 1999, **486**, 249.
15. Willems I, Konya Z, Colomer J F, Van Tendeloo G, Nagaraju N, Fonseca A and Nagy J B, *Chem Phys Lett.*, 2000, **317**(1-2), 71-76.

16. Benito P, Herrero M, Labajos F M, Rives V, Royo C, Latorre N and Monzon A, *Chem Eng J.*, 2009, **149(1-3)**, 455-462
17. Colomer J F, Stephen C, Lefrant S, Van Tendeloo G, Willems I, Konya Z, Fonseca A, Laurent Ch and Nagy J B, *Chem Phys Lett.*, 2000, **317(1-2)**, 83-89.
18. Qingwen L, Hao Y, Yan C, Jin Z and Zhongfan L, *J Mater Chem.*, 2002, **12**, 1179- 1183.
19. Tang S, Zhong Z, Xion Z, Sun L, Liu L, Lin J, Shen Z X and Tan K L, *Chem Phys Lett.*, 2001, **350(1-2)**, 19-26.
20. Wasyluk J, Perova T S, Lau D W M, Taylor M B, McCulloch D G and Stopford J, *Diamond Relat Mater.*, 2010, **19(5-6)**, 514-517.
21. Ballutaud D, Jomard F, Kociniowski T, Rzepka E, Girard H and Saada S, *Diamond Relat Mater.*, 2008, **17(4-5)**, 451-456.
22. Costa S, Brorowiak-Palen E, Kruszynska M, Bachmatiuk A and Kaenczuk R J, *Mater Sci Poland.*, 2008, **26(2)**, 433-441.